

# Antiangiogenic Effects of Doxazosin on Experimental Choroidal Neovascularization in Mice

Jiaxian Guo,<sup>1,2</sup> Xueting Luo,<sup>1,2</sup> Jian Liang,<sup>1,2</sup> Meichun Xiao,<sup>1,2</sup> and Xiaodong Sun<sup>1,2</sup>

## Abstract

**Purpose:** The present study was designed to evaluate the effects of doxazosin on experimental choroidal neovascularization (CNV) in mice.

**Methods:** Six- to 8-week-old male C57BL/6 mice were divided into a control group and a doxazosin-treated group (5 mg/kg, i.p., daily). Experimental CNV was induced by laser photocoagulation. Seven and 14 days after laser induction, fluorescein angiography, choroidal flat mounts, and histological studies were performed to evaluate the fluorescence leakage, area, and thickness of CNV lesions, respectively. In addition, western blot analysis was carried out to assess the inhibitory effects of doxazosin on the PI3K/Akt/mTOR signaling pathway and the expression levels of hypoxia-inducible factor 1 $\alpha$  (HIF-1 $\alpha$ ) and vascular endothelial growth factor (VEGF), which are involved in CNV model.

**Results:** Compared with the control group, the doxazosin-treated group demonstrated significantly less fluorescence leakage on day 7 and 14 after laser induction. Both the area and the thickness of CNV lesions in the doxazosin-treated group were significantly decreased. Mechanistically, PI3K/Akt/mTOR signaling pathway activation was significantly suppressed in the doxazosin-treated group. The expression of HIF-1 $\alpha$  and VEGF was also notably reduced by systemic doxazosin treatment.

**Conclusions:** Doxazosin exerts antiangiogenic actions in an experimental mouse model of CNV and may be a potential adjunctive therapy for neovascular age-related macular degeneration in humans.

**Keywords:** choroidal neovascularization, laser-induced, doxazosin, antiangiogenic

## Introduction

AGE-RELATED MACULAR DEGENERATION (AMD) is among the leading causes of severe visual impairment among elderly individuals in China and developed countries.<sup>1-3</sup> Clinically, AMD is divided into 2 types, dry and wet; the latter is also referred to as neovascular AMD and is characterized by the formation of choroidal neovascularization (CNV), which grows through Bruch's membrane into the subretinal space.<sup>4,5</sup> CNV is responsible for vision loss in AMD patients due to the exudates, hemorrhage, and fibrotic scarring of its newly formed hyperpermeable vessels.<sup>6,7</sup> Although the exact pathogenesis of CNV is complex and has not been fully elucidated, a growing body of clinical and experimental research implies a critical role for vascular endothelial growth factor (VEGF) in the occurrence and development of CNV.<sup>8,9</sup> Overexpression of VEGF promotes CNV development, whereas inhibition of VEGF leads to significant CNV suppression.<sup>10</sup> Therefore, anti-VEGF is a first-

line therapy for CNV treatment and successfully slows vision loss and even partially restores vision in certain patients with neovascular AMD.<sup>11,12</sup> However, some patients demonstrate poor responses or no response to anti-VEGF agents or are resistant to therapy after repeated treatment.<sup>13,14</sup> Long-term clinical follow-up indicates that many patients still experience visual loss after reaching a stable condition.<sup>15</sup> Besides, the risk of complications such as endophthalmitis and the high costs associated with multiple anti-VEGF injections are also drawbacks of current intravitreal anti-VEGF therapeutic regimens.<sup>16,17</sup> Therefore, an adjunctive therapeutic approach is desired for the treatment of neovascular AMD.

Doxazosin, a quinazoline compound, is an  $\alpha$ 1 adrenergic receptor blocker. It has long been prescribed to treat patients with benign prostatic hyperplasia and hypertension.<sup>18</sup> In recent years, the antitumor effects of doxazosin, particularly in prostatic cancer, have been described in a wide range of experimental studies.<sup>19,20</sup> Doxazosin not only directly stimulates

<sup>1</sup>Department of Ophthalmology, Shanghai General Hospital, Shanghai Jiao Tong University School of Medicine, Shanghai, China.

<sup>2</sup>Shanghai Key Laboratory of Ocular Fundus Diseases, Shanghai, China.

tumor cell apoptosis but also exerts antiangiogenic properties and inhibits tumor development by restraining neovascularization in corresponding tumor areas.<sup>21</sup> *In vitro*, doxazosin effectively inhibits adhesion, migration, and tube formation in human vascular endothelial cells and directly targets VEGF-mediated angiogenesis.<sup>22</sup> Furthermore, doxazosin suppresses neovascularization by regulating the PI3K/Akt/mTOR signaling pathway and hypoxia-inducible factor 1 $\alpha$  (HIF-1 $\alpha$ ) expression,<sup>23</sup> whose essential roles in CNV formation have been well characterized.<sup>24–26</sup> Therefore, doxazosin may be effective for the management of CNV.

In the present study, we investigate the effects of doxazosin in a laser-induced mouse CNV model to evaluate its potential for inhibition of CNV.

## Methods

### Animals

All animal experiments conformed to the Statement of the Association for Research in Vision and Ophthalmology for the Use of Animals in Ophthalmic and Vision Research. Male C57BL/6 mice aged 6–8 weeks were obtained from the Laboratory Animal Center of Shanghai General Hospital and maintained in a climate-controlled animal facility on a 12-h on/off light cycle. The mice were fed normal mouse chow and freely supplied with water and food.

### Drug

Doxazosin powder was purchased from Selleckchem (Houston, TX). The drug was dissolved in dimethyl sulfoxide (DMSO; Sigma, St. Louis, MO) at a concentration of 10 mg/mL and was diluted 50 times in 0.9% normal saline for *in vivo* studies. Doxazosin solution was stored at  $-20^{\circ}\text{C}$  and thawed immediately before administration. The solution was administered intraperitoneally to the mice daily at a dose of 5 mg/kg (ie, 0.5 mL solutions) from the day before laser induction to the end of the study.

### Laser-induced CNV mouse model

Mice were anesthetized with 2% sodium pentobarbital (Guge Biotech, Wuhan, China) through an intraperitoneal injection of 0.05 mL. Pupils were dilated with 5.0% tropicamide phenylephrine eye drops (Santen, Osaka, Japan). CNV was induced with a 532-nm laser system (Coherent, Inc., Santa Clara, CA) using a previously described protocol with modifications.<sup>27</sup> A coverslip was placed on the surface of the mouse cornea as a contact lens to view and focus on the retina. Laser spots were created in each eye using a slit-lamp delivery system with power of 120 mW, a spot size of 50  $\mu\text{m}$ , and a duration of 100 ms. Four lesions were created between the retinal vessels around the optical nerve head of each eye. The presence of a bubble at the time of laser application confirmed the sufficient rupture of Bruch's membrane to induce CNV. Subretinal hemorrhage induced by the laser was excluded from analysis.

### Fluorescence angiography

Fluorescein angiography was performed on day 7 and 14 after laser photocoagulation to evaluate the extent of CNV leakage. After mice were anesthetized and pupils were di-

lated as previously described, each mouse was subsequently injected intraperitoneally with 0.05 mL of 10% fluorescein sodium (Fluorescein; Alcon, Tokyo, Japan), and fundus angiogram photographs were taken using a digital fundus camera [Heidelberg Retina Angiograph (HRA), Vista, CA]. The captured images were analyzed using ImageJ software (National Institutes of Health, Bethesda, MD). The average signal intensity (brightness) of each CNV lesion with leakage was calculated as previously described in published studies.<sup>28</sup> The signal intensity for each pixel was represented as an arbitrary unit from 0 (darkest) to 1 (brightest). As a reference, the intensity within a nonphotocoagulated capillary area was defined as 0, and the intensity at the major branch of the retinal vein was defined as 1.<sup>28</sup>

### Choroidal flat mount

On day 7 and 14 after laser injury, mice were sacrificed by carbon dioxide exposure, and eyes were enucleated and fixed with 4% paraformaldehyde for 2 h. The retinal pigment epithelium (RPE)–choroid-sclera complex was obtained by removing the anterior segments and neurosensory retina. Approximately, 4–6 relaxing radial incisions were made to flatten the remaining eyecup. After blocking in phosphate-buffered saline (PBS) with 5% goat serum albumin (Beyotime, Shanghai, China) and 0.3% Triton X-100 (Solarbio, Beijing, China) for 1 h at room temperature, eyecups were incubated with isolectin B4 (1:500; Vector Laboratories, Burlingame, CA) overnight at  $4^{\circ}\text{C}$ . The eyecups were washed with PBS 3 times before they were flat-mounted with the RPE side facing up and coverslipped. CNV lesions were visualized using a blue argon laser wavelength (488 nm) with a fluorescence microscope (Olympus, Tokyo, Japan). CNV lesion areas were quantified with system software.

### Histological studies

Histological studies were carried out on day 7 and 14 after the laser induction of CNV to assess the thickness of CNV lesions. Eyes were enucleated and immersed in 4% paraformaldehyde for fixation, then processed for paraffin embedding. Serial sections with a thickness of 4  $\mu\text{m}$  were cut to determine the center of each CNV lesion, then mounted on glass slides. Sections were stained with hematoxylin and eosin (H&E) for light microscopy. Subsequent observations and analysis of CNV lesions in the H&E-stained sections were performed with a light microscopy (Olympus) and system software. The maximum CNV thickness, defined as the distance from the bottom of the choroidal layer to the top of the neovascular membrane, was assessed through the center of the laser photocoagulation spot at 200 $\times$  magnification.

### Western blot analysis

Western blot analysis was performed to investigate the inhibitory effects of doxazosin on the PI3K/AKT/mTOR signaling pathway and the expression of HIF-1 and VEGF. Protein extracts were obtained from the RPE-choroid-sclera complex 3 days after photocoagulation. RPE-choroid-sclera tissues were dissected, pooled in lysis buffer, and homogenized using a Vibra-Cell (Sonics & Materials, Newtown, CT). Then, the tissue lysates were centrifuged at 12,000 rpm for 10 min at  $4^{\circ}\text{C}$ , and the supernatants were separated for denaturation at  $99^{\circ}\text{C}$  and stored at  $-20^{\circ}\text{C}$ . Each sample was

electrophoresed on a 10% sodium dodecyl sulfate (SDS)–polyacrylamide gel and electroblotted onto a polyvinylidene fluoride (PVDF) membrane (Merck Millipore, Billerica, MA). After blocking nonspecific binding with 5% skim milk, the membranes were incubated with primary antibodies against phosphorylated Akt (1:1,000; Cell Signaling Technology, Beverly, MA), phosphorylated S6 (indicator for activation of mTOR, 1:1,000; Cell Signaling Technology), HIF-1 $\alpha$  (1:1,000; Proteintech, Chicago, IL), VEGF (1:1,000; Abcam, Cambridge, MA), and  $\beta$ -Actin (1:1,000; Cell Signaling Technology) at 4°C overnight. Membranes were then incubated with horseradish peroxidase-conjugated secondary antibodies (1:5,000; Proteintech) for 1 h at room temperature. The signals were visualized and recorded using an ECL Kit (Merck Millipore) and a molecular imaging system (Amersham Imager 600; GE Healthcare, Buckinghamshire, United Kingdom). Protein expression levels were normalized to the corresponding expression of  $\beta$ -actin as a control and expressed as arbitrary units.

### Statistical analysis

All data are expressed as mean  $\pm$  standard deviation. Statistical analysis was performed using GraphPad Prism for Windows (Version 5.01; GraphPad Software, Inc., San Diego, CA). The results for the 2 groups were then compared using Student's *t*-test to assess the effects of drug treatment. Statistical significance was defined as  $P < 0.05$ .

## Results

### Fluorescein angiography

According to our fluorescein angiographic analysis 7 days after the photocoagulation of experimental CNV, the average

fluorescein intensity scores of the control group and doxazosin-treated group were  $0.7435 \pm 0.0311$  and  $0.5172 \pm 0.0282$ , respectively. There were statistically significant differences between the doxazosin-treated group ( $P < 0.001$ ) and the control group. Similarly, 14 days after laser induction, the fluorescein signal intensity scores of the control and doxazosin-treated groups were  $0.8041 \pm 0.0353$  and  $0.5808 \pm 0.0414$ , respectively ( $P < 0.001$ ), also indicating a significant decline after treatment (Fig. 1).

### Choroidal flat mount

CNV lesion area was measured by performing choroidal flat mounts to evaluate the inhibitory effects of doxazosin treatment on experimental CNV (Fig. 2). Seven days after laser injury, doxazosin-treated mice exhibited a significant decrease in CNV lesion area ( $12.43 \pm 0.84 \times 10^3 \mu\text{m}^2$ ) compared with control mice ( $21.81 \pm 1.49 \times 10^3 \mu\text{m}^2$ ). CNV was notably suppressed by doxazosin treatment after 14 days as well. The lesion areas observed for the doxazosin-administered group and the control group were  $10.03 \pm 0.78$  and  $20.11 \pm 1.72 \times 10^3 \mu\text{m}^2$ , respectively. The doxazosin-treated group showed significant CNV lesion area reductions of 43% and 50% on day 7 and 14, respectively, compared to the control group.

### Histological studies

Representative H&E-stained sections of CNV lesions 7 and 14 days after laser photocoagulation are shown in Fig. 3. Dome-like CNV complexes consisting of retinal pigment epithelial cells, pigment clumps, and proliferative fibrovascular tissues were observed. On day 7 after laser induction, the average CNV thicknesses of the treated group and control group were  $29.30 \pm 2.15$  and  $42.39 \pm 2.18 \mu\text{m}$ , respectively,

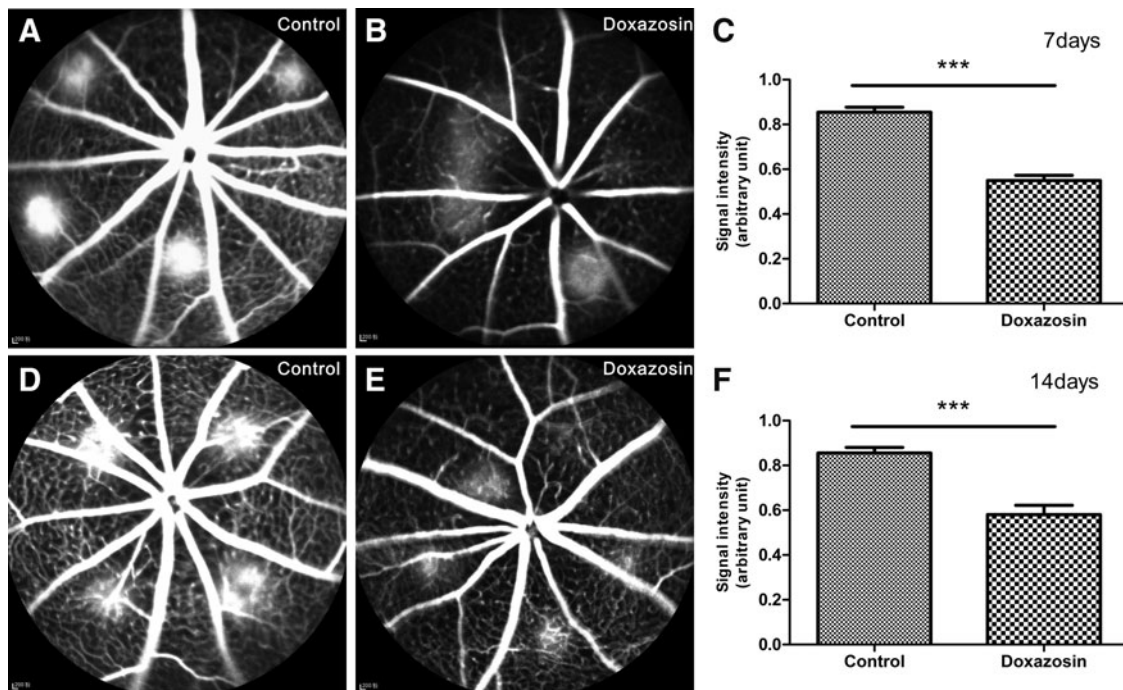


**FIG. 1.** Representative fluorescein angiographic images of laser-induced CNV on day 7 and 14 after photocoagulation. (A) Control group on day 7; (B) doxazosin-treated group on day 7; (D) control group on day 14; and (E) doxazosin-treated group on day 14. Fluorescein leakage of the doxazosin-treated group was significantly decreased compared with the control group (C, F: \*\*\* $P < 0.001$ ). CNV, choroidal neovascularization.

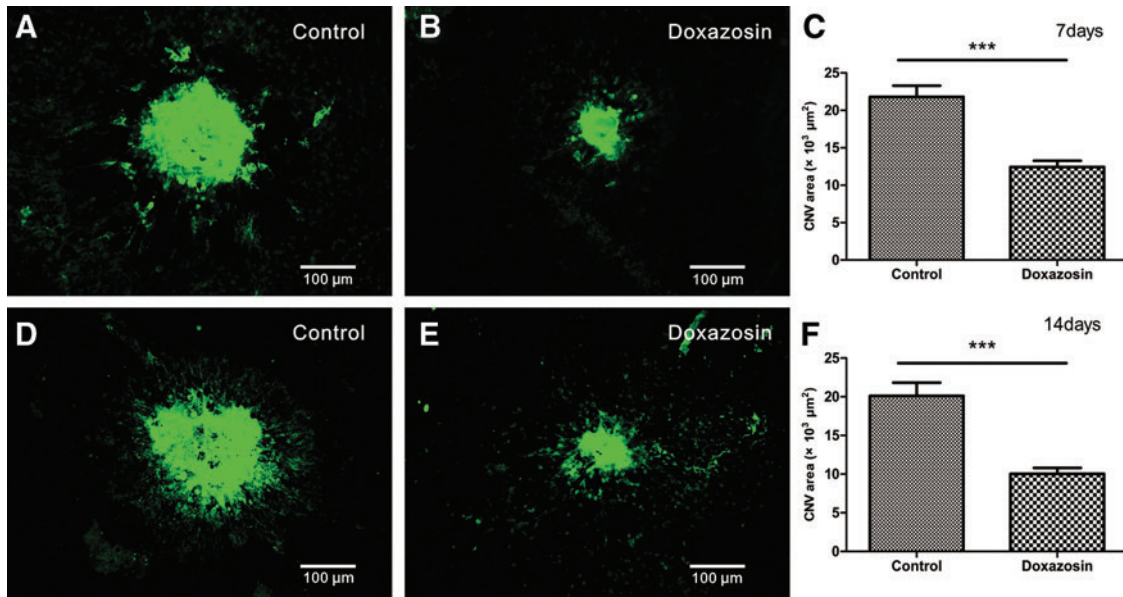


**FIG. 2.** Images of choroidal flat mounts 7 and 14 days after laser injury. (A) Control group after 7 days; (B) doxazosin-treated group after 7 days; (D) control group after 14 days; and (E) doxazosin-treated group after 14 days. CNV lesions were assessed quantitatively. The administration of doxazosin significantly suppressed laser-induced CNV lesion area size in mice (C, F: \*\*\* $P < 0.001$ ). Scale bar, 100 μm.

while on day 14, the average thicknesses were  $28.92 \pm 1.11$  and  $41.10 \pm 2.20$  μm. According to the measurements and statistical analysis results, CNV lesions in the doxazosin-treated group were significantly less thick compared to the control group.

#### Western blot analysis

We next investigated whether the administration of doxazosin leads to the inhibition of HIF-1α and VEGF protein levels and activation of the PI3k/Akt/mTOR signaling pathway in our experimental mouse CNV model. Three days

after laser induction, HIF-1α and VEGF expression levels were decreased in the doxazosin-treated group compared with the control group (as shown in Fig. 4). Furthermore, our results also demonstrated that doxazosin treatment was capable of reducing the expression levels of p-Akt and p-S6 in RPE-choroid-sclera tissues 3 days after laser injury.

#### Discussion

In the present study, we investigated the antiangiogenic activity of doxazosin in a laser-induced mouse CNV model

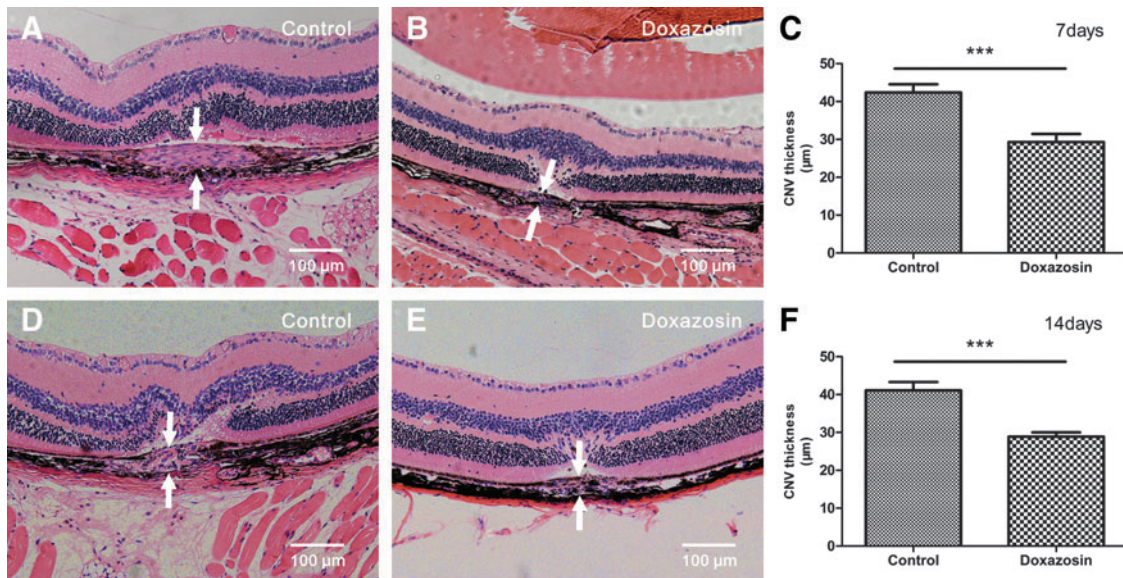


**FIG. 3.** Effects of doxazosin on CNV lesion thickness 7 and 14 days after laser induction. Light micrographs of H&E-stained sections of CNV lesions in the control group after 7 days (A), in the doxazosin-treated group after 7 days (B), in the control group after 14 days (D), and in the doxazosin-treated group after 14 days (E) are shown. CNV thickness in the doxazosin-treated group was significantly lower compared to the control group (C, F: \*\*\* $P < 0.001$ ). The distance between the two white arrows indicates CNV thickness. Scale bar, 100 μm. H&E, hematoxylin and eosin.

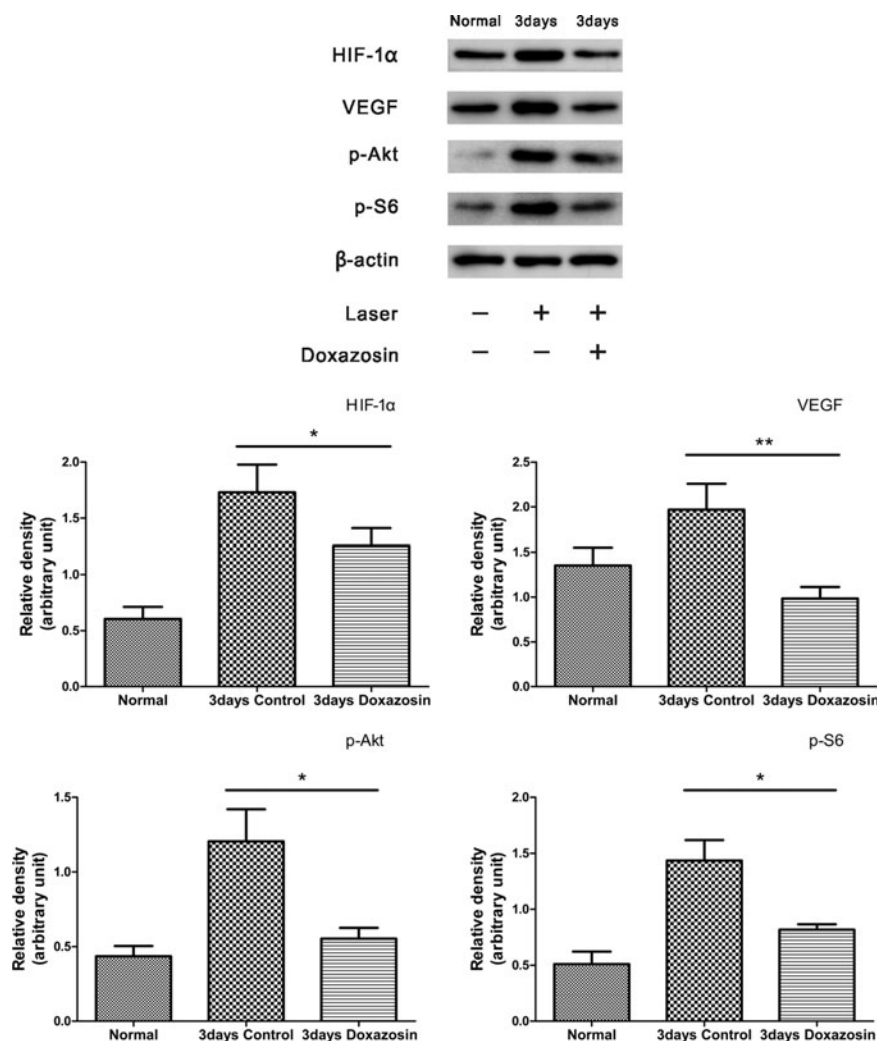


**FIG. 4.** Quantification of HIF-1 $\alpha$ , VEGF, and p-Akt and p-S6 expression levels in the retinal pigment epithelium-choroidal-scleral complex 3 days after laser injury. \* $P < 0.05$ , \*\* $P < 0.01$  compared to the control group. HIF-1 $\alpha$ , hypoxia-inducible factor 1 $\alpha$ ; VEGF, vascular endothelial growth factor.

and demonstrated the ability of doxazosin, at a dose of 5 mg/kg/day, to effectively inhibit experimental CNV.

According to our experimental results, the systemic administration of doxazosin suppressed fluorescence leakage due to CNV compared with the control group, as determined by fluorescein angiography. CNV lesion areas, measured in choroidal flat mounts, also significantly decreased after doxazosin treatment. In addition, doxazosin decreased the thickness of CNV lesions in our histological analyses. All the findings indicated that doxazosin could reduce the formation and development of experimental CNV. Furthermore, HIF-1 $\alpha$  and VEGF expression levels were suppressed by doxazosin treatment. Based on the results of our western blot analysis, the inhibitory effects of doxazosin on experimental CNV may involve blocked activation of the PI3K/AKT/mTOR signaling pathway. Overall, doxazosin has significant potential as a therapeutic agent for CNV treatment.

Recently, the potent antiangiogenic activity of doxazosin has elicited exciting discussions in the research community. Doxazosin was shown to suppress prostate cancer vascularity by decreasing VEGF in clinical specimens.<sup>29</sup> As we all know, CNV in combination with neovascular AMD is characterized as an angiogenic disease, and the laser-induced mouse CNV model used in our experiments shares many important features with naturally occurring CNV in humans, such as the

disruption of Bruch's membrane, elevated VEGF levels, and CNV formation.<sup>7</sup> Based on our data, doxazosin exerts potent antiangiogenic effects in the CNV model, which is consistent with previous observations in other fields.

The PI3k/Akt/mTOR signaling pathway regulates a broad range of cellular processes, including survival, proliferation, growth, and metabolism, in numerous cell systems.<sup>30</sup> It is also well established that activation of the PI3k/Akt/mTOR signaling cascade plays a pivotal role in promoting angiogenesis, both in normal tissues and in cancers; increases the secretion of VEGF, a validated angiogenic factor, through HIF-1 $\alpha$ ; and partially regulates its significant effects on angiogenesis.<sup>31</sup> Specifically, PI3k/Akt/mTOR is also upstream of HIF-1 $\alpha$  and VEGF in experimental CNV.<sup>24</sup> Conversely, inhibition of PI3k/Akt/mTOR signaling pathway significantly suppresses vascular leakage and decreases CNV lesion size.<sup>25</sup> Therefore, the PI3k/Akt/mTOR signaling pathway is a regulator of laser-induced CNV angiogenic processes.

Notably, doxazosin exerts antiangiogenic effects by inhibiting activation of the PI3k/Akt/mTOR signaling pathway in human umbilical vein endothelial cells *in vitro*.<sup>23</sup> Doxazosin also suppresses HIF-1 $\alpha$  and VEGF expression in ovarian carcinoma cells.<sup>23</sup> Thus, the blockade of HIF-1 $\alpha$  and VEGF elevation and the PI3k/Akt/mTOR signaling pathway activation may explain the inhibitory effects of doxazosin on

experimental CNV. Indeed, our data are consistent with this hypothesis. According to our western blot analysis, doxazosin suppressed HIF-1 $\alpha$  and VEGF expression in RPE-choroid-sclera tissues 3 days after laser induction. Furthermore, it has also been found that doxazosin inhibits the expression of p-Akt and p-S6. Overactivation of the PI3K/Akt/mTOR pathway is characterized by the increased production of p-Akt and p-S6.<sup>32</sup> Thus, reduced Akt and S6 phosphorylation, as observed in our results, indicates suppression of the PI3K/Akt/mTOR signaling pathway by doxazosin in the CNV model. Studies have shown that HIF-1 $\alpha$  is an important regulator of VEGF secretion mainly by RPE cells.<sup>33,34</sup> We suspect doxazosin may inhibit HIF-1 $\alpha$  protein levels by blocking the PI3K/AKT/mTOR pathway and, subsequently, reducing VEGF expression mainly in RPE cells. However, the specific underlying mechanism still requires further investigation.

Doxazosin is an oral drug that has been used clinically for years. The effects of doxazosin on angiogenesis in the laser-induced mouse CNV model suggest a plausible extension of its clinical use from benign prostate hyperplasia symptoms and hypertension management to CNV prevention. It would be expedient to repurpose this drug as an antiangiogenic agent because it has already undergone toxicity testing in animals and humans and exhibits a good safety profile.

However, whether doxazosin is beneficial to pretreated CNV lesions, even with scars, is unclear and worth concerning for future investigations. Formation of fibrotic scars may be one of the major mechanisms of inadequate response or resistance to anti-VEGF treatment. Several studies have indicated that doxazosin treatment attenuates liver fibrosis.<sup>35</sup> But to our knowledge, there are no published studies regarding the effect of doxazosin on fibrotic scars related to CNV, which may be a promising research area in the future. The relationship between doxazosin and other important cytokines involved in experimental CNV remains unclear. Future studies are required to explore whether other downstream cytokines are involved in the mechanism underlying doxazosin-induced inhibition of experimental CNV. In addition, further efforts are required to determine the optimal dosage and delivery methods.

In conclusion, doxazosin exhibited potent antiangiogenic properties and significantly inhibited CNV progression in a laser-induced mouse model. Therefore, it may serve as a valuable candidate drug for the treatment of CNV in clinical practice. However, further investigation of doxazosin is warranted before its clinical application in patients with CNV.

## Acknowledgments

The authors thank Dr. Yu Chen at the Shanghai University of Traditional Chinese Medicine for valuable guidance on experimental design and helpful scientific instructions and discussions throughout the whole experiment. This research was supported by The National Science Fund for Distinguished Young Scholars of China (81425006); the Shanghai Science and Technology Innovation Project (1341195400); and the Program of Subject Chief Scientists of the Shanghai Health System (XBR2013081).

## Author Disclosure Statement

No competing financial interests exist.

## References

1. Ye, H., Zhang, Q., Liu, X., et al. Prevalence of age-related macular degeneration in an elderly urban Chinese population in China: the Jiangning Eye Study. *Invest. Ophthalmol. Vis. Sci.* 55:6374–6380, 2014.
2. Congdon, N., O'Colmain, B., and Klaver, C.C. Causes and prevalence of visual impairment among adults in the United States. *Arch. Ophthalmol.* 122:477–485, 2004.
3. Jager, R.D., Mieler, W.F., and Miller, J.W. Age-related macular degeneration. *N. Engl. J. Med.* 358:2606–2617, 2008.
4. Freund, K.B., Yannuzzi, L.A., and Sorenson, J.A. Age-related macular degeneration and choroidal neovascularization. *Am. J. Ophthalmol.* 115:786–791, 1993.
5. Lim, L.S., Mitchell, P., Seddon, J.M., et al. Age-related macular degeneration. *Lancet.* 379:1728–1738, 2012.
6. Roth, F., Bindewald, A., and Holz, F.G. Keypathophysiological pathways in age-related macular disease. *Graefes Arch. Clin. Exp. Ophthalmol.* 242:710–716, 2004.
7. Noël, A., Jost, M., Lambert, V., et al. Anti-angiogenic therapy of exudative age-related macular degeneration: current progress and emerging concepts. *Trends Mol. Med.* 13:345–352, 2007.
8. Bressler, S.B. Introduction: understanding the role of angiogenesis and antiangiogenic agents in age-related macular degeneration. *Ophthalmology.* 116:S1–S7, 2009.
9. Ishibashi, T., Hata, Y., Yoshikawa, H., et al. Expression of vascular endothelial growth factor in experimental choroidal neovascularization. *Graefes Arch. Clin. Exp. Ophthalmol.* 235:159–167, 1997.
10. Spilisbury, K., Garrett, K.L., Shen, W.Y., et al. Overexpression of vascular endothelial growth factor (VEGF) in the retinal pigment epithelium leads to the development of choroidal neovascularization. *Am. J. Pathol.* 157:135–144, 2000.
11. Özkiris, A. Anti-VEGF agents for age-related macular degeneration. *Expert. Opin. Ther. Pat.* 20:103–118, 2010.
12. Nguyen, D.H., Luo, J., Zhang, K., et al. Current therapeutic approaches in neovascular age-related macular degeneration. *Discov. Med.* 15:343–348, 2013.
13. Yang, S., Zhao, J., and Sun, X. Resistance to anti-VEGF therapy in neovascular age-related macular degeneration: a comprehensive review. *Drug Des. Devel. Ther.* 10:1857–1867, 2016.
14. Arcinue, C.A., Ma, F., Barteselli, G., et al. One-year outcomes of aflibercept in recurrent or persistent neovascular age-related macular degeneration. *Am. J. Ophthalmol.* 159:426–436, 2015.
15. Bhisitkul, R.B., Desai, S.J., Boyer, D.S., et al. Fellow eye comparisons for 7-year outcomes in Ranibizumab-treated AMD subjects from ANCHOR, MARINA, and HORIZON (SEVEN-UP study). *Ophthalmology.* 123:1269–1277, 2016.
16. Gragoudas, E.S., Adamis, A.P., Cunningham Jr., E.T., et al. Pegaptanib for neovascular age-related macular degeneration. *N. Engl. J. Med.* 351:2805–2816, 2004.
17. Sampat, K.M., and Garg, S.J. Complications of intravitreal injections. *Curr. Opin. Ophthalmol.* 21:178–183, 2010.
18. Park, M.S., Kim, B.R., Kang, S., et al. The antihypertension drug doxazosin suppresses JAK/STATs phosphorylation and enhances the effects of IFN- $\alpha/\gamma$ -induced apoptosis. *Genes Cancer.* 5:470–479, 2014.
19. Sakamoto, S., and Kyprianou, N. Targeting anoikis resistance in prostate cancer metastasis. *Mol. Aspects Med.* 31:205–214, 2010.
20. Gaelzer, M.M., Coelho, B.P., de Quadros, A.H., et al. Phosphatidylinositol 3-Kinase/AKT pathway inhibition by

- doxazosin promotes glioblastoma cells death, upregulation of p53 and triggers low neurotoxicity. *PLoS One*. 11: e0154612, 2016.
21. Bilbro, J., Mart, M., and Kyprianou, N. Therapeutic value of quinazoline-based compounds in prostate cancer. *Anticancer Res*. 33:4695–4700, 2013.
  22. Keledjian, K., Garrison, J.B., and Kyprianou, N. Doxazosin inhibits human vascular endothelial cell adhesion, migration, and invasion. *J. Cell. Biochem*. 94:374–388, 2005.
  23. Park, M.S., Kim, B.R., Dong, S.M., et al. The antihypertension drug doxazosin inhibits tumor growth and angiogenesis by decreasing VEGFR-2/Akt/mTOR signaling and VEGF and HIF-1 $\alpha$  expression. *Oncotarget*. 5:4935–4944, 2014.
  24. Yang, X.M., Wang, Y.S., Zhang, J., et al. Role of PI3K/Akt and MEK/ERK in mediating hypoxia-induced expression of HIF-1 $\alpha$  and VEGF in laser-induced rat choroidal neovascularization. *Invest. Ophthalmol. Vis. Sci*. 50:1873–1879, 2009.
  25. Ma, J., Sun, Y., López, F.J., et al. Blockage of PI3K/mTOR pathways inhibits laser-induced choroidal neovascularization and improves outcomes relative to VEGF-A suppression alone. *Invest. Ophthalmol. Vis. Sci*. 57:3138–3144, 2016.
  26. André, H., Tunik, S., Aronsson, M., et al. Hypoxia-inducible factor-1 $\alpha$  is associated with sprouting angiogenesis in the murine laser-induced choroidal neovascularization model. *Invest. Ophthalmol. Vis. Sci*. 56:6591–6604, 2015.
  27. Shah, R.S., Soetikno, B.T., Lajko, M., et al. A mouse model for laser-induced choroidal neovascularization. *J. Vis. Exp*. 106:e53502, 2015.
  28. Rho, C.R., Kang, S., Park, K.C., et al. Antiangiogenic effects of topically administered multiple kinase inhibitor, motesanib (AMG 706), on experimental choroidal neovascularization in mice. *J. Ocul. Pharmacol. Ther*. 31:25–31, 2015.
  29. Keledjian, K., Borkowski, A., Kim, G., et al. Reduction of human prostate tumor vascularity by the  $\alpha$ 1-adrenoceptor antagonist terazosin. *Prostate*. 48:71–78, 2001.
  30. Shaw, R.J., and Cantley, L.C. Ras, PI(3)K and mTOR signalling controls tumour cell growth. *Nature*. 441:424–430, 2006.
  31. Karar, J., and Maity, A. PI3K/AKT/mTOR pathway in angiogenesis. *Front. Mol. Neurosci*. 4:51, 2011.
  32. Su, H., Gu, Y., Li, F., et al. The PI3K/AKT/mTOR signaling pathway is overactivated in primary aldosteronism. *PLoS One*. 8:e62399, 2013.
  33. Forooghian, F., Razavi, R., Timms, L. Hypoxia-inducible factor expression in human RPE cells. *Br. J. Ophthalmol*. 91:1406–1410, 2007.
  34. Zhu, J., Wang, Y.S., Zhang, J., et al. Focal adhesion kinase signaling pathway participates in the formation of choroidal neovascularization and regulates the proliferation and migration of choroidal microvascular endothelial cells by acting through HIF-1 and VEGF expression in RPE cells. *Exp. Eye Res*. 88:910–918, 2009.
  35. Muñoz-Ortega, M.H., Llamas-Ramírez, R.W., Romero-Delgado, N.I., et al. Doxazosin treatment attenuates carbon tetrachloride-induced liver fibrosis in hamsters through a decrease in transforming growth factor beta secretion. *Gut Liver*. 10:101–108, 2016.

Received: September 26, 2016  
Accepted: October 29, 2016

Address correspondence to:  
Prof. Xiaodong Sun  
Department of Ophthalmology  
Shanghai General Hospital  
Shanghai JiaoTong University School of Medicine  
NO. 100, Haining Road  
Shanghai 200080  
China

E-mail: xdsun@sjtu.edu.cn